

## Off-Axis Co-Sputtered YBCO and CeO<sub>2</sub> Thin Films

E. J. Cukauskas, L. H. Allen, and J. Pond  
Naval Research Laboratory, Washington, DC 20375

**Abstract**—We have investigated the properties of off-axis co-sputtered films of YBCO and CeO<sub>2</sub> having CeO<sub>2</sub> concentrations up to 43%. Morphology investigations suggest that films with more than 29% CeO<sub>2</sub> may consist of a new material phase.  $T_c$  and resistance ratio decreased with increasing CeO<sub>2</sub> concentration. Degradation of  $T_c$  after photoresist processing the films was observed and reversed by a 20 minute oxygen plasma etch. The temperature dependence of the critical current near  $T_c$  showed two power law dependence regions with a crossover near  $0.99 T_c$  for films having low concentrations of CeO<sub>2</sub>.  $I_c$ 's were decreased by small applied magnetic fields, and for some samples the response was observed to increase at lower temperature. For a sample having 26% CeO<sub>2</sub>, a 40% reduction in critical current was observed for a 2 Gauss applied field. This response indicates that this may be a candidate material for the development of Josephson vortex flow devices.

### I. INTRODUCTION

Three-terminal superconducting devices which rely on the motion of magnetic vortices is an area of high temperature superconducting (HTS) electronics receiving recent attention[1]-[4]. The successful development of a three-terminal HTS device having gain can have a significant impact on the viability of superconducting electronics. The Superconducting Vortex Flow Transistor (SVFT) has been demonstrated in both low  $T_c$  and HTS materials technology. Its speed and frequency response are dependent on the materials properties and the kind of vortices (Abrikosov or Josephson) responsible for the device transport.

Single layer vortex flow devices require a region of weakly pinned vortices for controlling the transport with a small external magnetic field. Weak vortex pinning can be realized in a device by incorporating an array of weak-links into the structure or by the use of a grain boundary Josephson junction. In our approach, we have developed a composite material which appears to consist of superconducting grains with non-superconducting grain boundaries that have the characteristic of weak vortex pinning. Weak pinning makes this material a candidate for vortex flow device development.

Recently, we reported a technique for depositing granular metal matrix composites of YBa<sub>2</sub>Cu<sub>3</sub>O<sub>7</sub> (YBCO) and gold or silver [5]-[7]. These composites consist of arrays of YBCO grains coupled together by regions of gold or silver and exhibit transport characteristics similar to those of Superconductor/Normal/Superconductor (SNS) junctions. Significant critical current reduction was observed for applied magnetic fields less than 100 Gauss. The electrical characteristics of these materials were dependent upon the substrate. In this paper, we focus our work on a new YBCO composite film prepared by off-axis co-sputtering YBCO and CeO<sub>2</sub>.

### II. SAMPLE PREPARATION

The YBCO/CeO<sub>2</sub> films were co-sputtered onto (100) MgO using a multi-target off-axis sputtering system described elsewhere [8]. All films were deposited at a substrate holder temperature of 680°C in the flowing deposition gas mixture of argon, oxygen and hydrogen. The gas flow rates were set to 54 sccm for argon, 34 sccm for oxygen, and 11 sccm for hydrogen. After stabilizing the gas flow, the chamber pressure was set to 150 microns for film deposition. The targets were pre-sputtered for 30 minutes at 0.45 A DC for the face-to-face YBCO targets and the CeO<sub>2</sub> target at the appropriate rf power level for the desired composition. The film composition was calculated from the YBCO and CeO<sub>2</sub> deposition rates and time. The films were sputtered for four hours which resulted in a film thickness ranging from approximately 160 to 280 nm. After deposition, the film was cooled to ambient temperature in one atmosphere of oxygen. Silver contact pads were thermally evaporated through a shadow metal mask prior to sample characterization. A series of YBCO/CeO<sub>2</sub> films were deposited using these conditions each at a different CeO<sub>2</sub> rf power level yielding films having CeO<sub>2</sub> volume concentrations from 0% to 43% for rf power levels up to 150 W.

### III. MORPHOLOGICAL PROPERTIES

We have studied the microstructure of the composite films for several concentrations of CeO<sub>2</sub> using x-ray diffraction (XRD) and scanning electron microscopy (SEM). The observed spectra for plain YBCO was predominantly c-axis oriented with sharp peaks corresponding to the YBCO (0 0 1) reflections. For small CeO<sub>2</sub> concentrations, the peaks shifted to lower angles and became distorted and broad. At 28.6% CeO<sub>2</sub> concentration we observed an abrupt change in the spectra. The spectra had three peaks, two intense, sharp peaks at 23.1° and 47.2° and a small one at 73.6°. These peaks were significantly shifted from the closest YBCO c-axis peaks with the peak at 47° being more than 0.5° higher. The line shape and position of the (0 0 6) for three CeO<sub>2</sub> concentrations are illustrated in Fig. 1. The spectra for the 28.6% CeO<sub>2</sub> film may represent a different material phase, and by fitting the new peaks for a lattice parameter, we obtain a value of  $3.863 \text{ \AA} \pm 0.005 \text{ \AA}$ . This is very close to the lattice parameter for YBCO in either the orthorhombic or tetragonal phase and also to the (1 1 1) planar spacing for a cerium perovskite, BaCeO<sub>3</sub> [9],[10]. To identify this phase, we compared the intensity ratio of the 47° peak to the 23° (peak which is 12) to the value for the YBCO orthorhombic phase (3) and the tetragonal phase [9]. Neither fits, and we could not find a ratio value for BaCeO<sub>3</sub> in the literature. More information such as off-axis XRD scans may be necessary to identify this phase. The SEM micrograph a plain YBCO film shows c-axis oriented grains and a smooth surface with a few

Manuscript received August 27, 1996

This work was supported by the Office of Naval Research

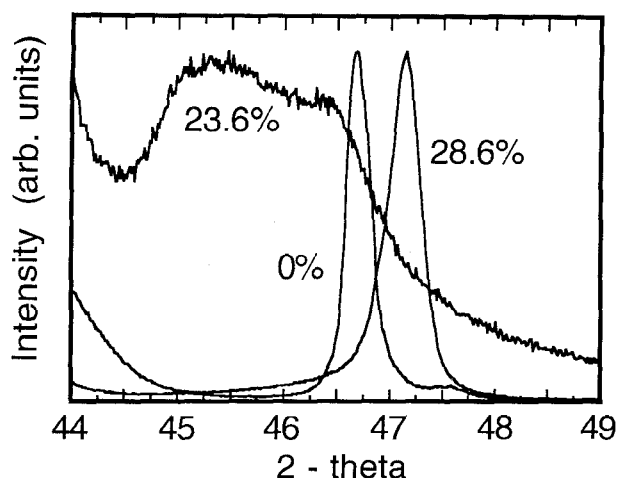


Fig. 1 The (0 0 6) x-ray diffraction peak for YBCO/CeO<sub>2</sub> films having the indicated concentrations.

scattered outcroppings and several voids. Grain boundaries are difficult to resolve, but the average grain size is estimated between 0.5 to 1  $\mu\text{m}$ . As the amount of CeO<sub>2</sub> was increased in the film, we observed more outcropping grains, and the background grains were less oriented but they still have a similar appearance to the YBCO grains. The significant change in the x-ray spectra of the 28.6% was also reflected in the SEM micrograph illustrated in Fig. 2. The background is no longer smooth, but is an interlocking mesh of smaller grains, 100 nm to 200 nm in size. The grains are clearly oriented in the plane of the film and as they make up the bulk of the film, are probably the new phase suggested by XRD.

#### IV. ELECTRICAL CHARACTERIZATION

The electrical characterization of the samples was performed in a closed cycle helium refrigerator. The samples and a silicon diode thermometer were heat sunk by indium foil to the refrigerator's cold stage. The as-sputtered films were characterized for room temperature resistance ( $R_{300\text{K}}$ ),  $T_c$ ,

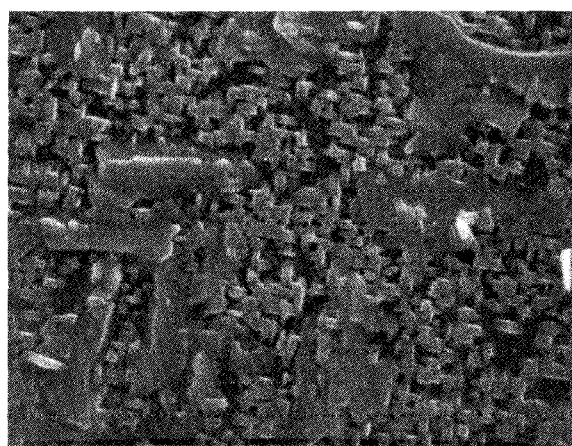


Fig. 2 The SEM micrograph of a YBCO/CeO<sub>2</sub> film having 28.6% CeO<sub>2</sub>.

transition width ( $\Delta T_c$ ), and resistance ratio (RR).  $T_c$  was defined as the temperature at which the sample resistance became less than 1 m $\Omega$ ,  $\Delta T_c$  as the temperature interval between the 10 and 90% resistance points just below the transition onset, and RR as the ratio of the resistance at 295 K and 100 K. The  $T_c$  of the as-sputtered films decreased and the transition width increased as more CeO<sub>2</sub> was incorporated into the films. These observations are consistent with a random de-coupling of the superconducting grains as the CeO<sub>2</sub> was increased, producing a range of  $T_c$ 's that broadened the transition.  $T_c$  rapidly falls off above approximately 13% CeO<sub>2</sub>, and  $R_{300\text{K}}$  rises sharply at about 30% CeO<sub>2</sub>. As-sputtered films with more than 23% CeO<sub>2</sub> were non-superconducting. After characterization, the films were then scribed or etched into a bridge geometry for critical current measurements and magnetic field response.

We found a substantial degradation in  $T_c$  and an increase in resistance after processing samples using standard photolithography and wet chemical etching. Some samples became non-superconducting, however after subjecting them to an oxygen plasma etch, they became superconducting.

To gain insight into the effect of the oxygen plasma etch on the films, a 15% CeO<sub>2</sub> sample was patterned with photoresist and ion milled into a 1 mm wide bridge and subjected to an oxygen plasma for 20 minutes in a barrel etcher.  $T_c$  measurements after the oxygen plasma etch showed a significant improvement in  $T_c$  and a reduction in resistance over the values measured prior to the etch. The as-sputtered film  $T_c$  was 68.3 K, and after ion milling had degraded to 51.3 K. However, after the oxygen plasma etch,  $T_c$  increased to 75.0 K and  $R_{300\text{K}}$  changed from 198  $\Omega$  to 60.7  $\Omega$ .

Sufficient energy existed in the oxygen plasma to cause the silver contact pads to become discontinuous. SEM micrographs showed the silver became an array of spiral-shaped columnar grains several hundred nm in diameter. This suggests that the plasma etch may also have caused material movement within the YBCO grain boundaries leading to improved superconducting properties.

These results are compatible with improved grain boundaries but give no evidence regarding the quality of the grains. We used a microwave inductive  $T_c$  measurement technique being developed by Pond et al. [11] to study the effect of the oxygen plasma process. The technique was applied to a film containing 16.6% CeO<sub>2</sub> both before and after photolithographic processing. The results were compared to the resistive and 10 kHz inductive  $T_c$  measurements. Table I summarizes the results.

TABLE I

SUMMARY OF THE INDUCTIVE AND RESISTIVE $T_c$ MEASUREMENTS		
as-sputtered	61.7K	10 kHz Ind $T_c$
as-sputtered & O <sub>2</sub> pe	64.3 K	10 kHz Ind $T_c$
as-sputtered & O <sub>2</sub> pe	79.4 K	2 GHz Ind $T_c$
patterned 150 $\mu$ bar	78 K	2 GHz Ind $T_c$
patterned 150 $\mu$ bar	64.6 K	$T_c$ @ R = 0

The inductive (Ind)  $T_c$  is defined as the onset of the inductive transition. An oxygen plasma etch (O<sub>2</sub> pe) was performed after each processing step. The 10 kHz inductive  $T_c$  onset agrees well with the 64.6 K resistive  $T_c$ . The 2 GHz inductive  $T_c$  onset at 78 K occurs just below the onset of the

resistive transition. These results support that the oxygen plasma etch improved the grain boundaries and there was little degradation to the grains from the ion milling.

The oxygen plasma etched samples were characterized by  $T_c$ ,  $\Delta T_c$ , RR,  $R_{300K}$ ,  $I_c(T)$  near  $T_c$ , and response to small applied magnetic fields. The results of selected samples are listed in Table II.  $I_c$  was taken as that value of current which showed a clear departure ( $\sim 0.1 \mu V$ ) from the voltage noise fluctuations. A graphical representation of the transition's mid-point and its  $\Delta T_c$  as a function of  $CeO_2\%$  is shown by Fig. 3. The 10 and 90% resistance points are indicated by the error bars.

The temperature dependence of the critical current near  $T_c$  can suggest the nature of the inter-granular coupling for polycrystalline films [12]-[14]. In these YBCO/ $CeO_2$  films, our goal is to modify the grain boundaries or incorporate an insulating material between the YBCO grains. For the YBCO/ $CeO_2$  films, we expect to see a departure from the  $3/2$  power law dependence typically observed for plain YBCO.

The critical current of the bridges was measured in the vicinity of  $T_c$  and fit to a power law dependence of the form  $I_c = I_0 (1-t)^n$ , where  $t = T/T_c$  is the reduced temperature. Very close to  $T_c$ , increments of temperature as small as 0.05 K were taken for some samples, however, noise fluctuations prohibited these kinds of measurements for all samples. The value of  $T_c$  used to calculate the reduced temperature was taken as the temperature for which no discernible critical current existed or by extrapolating the  $I_c$  vs.  $T$  data to zero. Using this value of  $T_c$ , a plot of  $\log(I_c)$  vs.  $\log(1-t)$  was made and fit to  $(1-t)^n$ . Figure 4 illustrates the least squares fit to the temperature dependence of the critical current for a 20%  $CeO_2$  sample. The values of the exponent "n" at high and low temperatures,  $n_c$  and  $n_s$ , and the crossover point  $t_{cross}$  are tabulated in Table II for each sample whose critical current was studied. For  $t < t_{cross}$  (higher  $I_c$ ), the samples had "n" values nearly two or greater except for the samples made with 23% and 28.6%  $CeO_2$ . For this temperature region, the power law fit yielded exponents more like those associated with SNS intergranular coupling rather than linear SIS theory of Ambegaokar-Baratoff or the  $3/2$  power of the Ginzburg-

Landau theory [15], [16]. The  $I_c$  vs.  $t$  characteristics of each sample showed a distinct change in slope at  $t_{cross}$ , which was very close to 1. The power law exponent is 0.5 to 1 for most samples for  $t_{cross} < t < 1$ . The value of  $t_{cross}$  becomes smaller (farther from  $T_c$ ) for the higher concentrations of  $CeO_2$ .

Several measurements of the effect of small applied magnetic fields on the critical current were taken on the bridges. A magnetic field up to 150 Gauss was applied to the samples by a solenoid magnet having a length to diameter ratio of two and positioned such that the sample was centered with the magnetic field perpendicular to the surface of the film.  $I_c$  measurements were taken at fixed temperatures and several values of the applied magnetic field. A 23.1%  $CeO_2$  sample showed a 13% reduction in  $I_c$  at a 0.6 reduced temperature by a 5 Gauss magnetic field. At lower temperatures, we observed a greater reduction in  $I_c$  for the same field, an effect which is not associated with Abrikosov vortices but with Josephson vortices. For some samples we studied the sensitivity of  $I_c$  for small fields of several Gauss.

If the field response is a result of Josephson vortices, then the response should be greater at lower fields where the  $\sin(x)/x$  function of  $I_c(B)$  in a junction varies the most. The reduced critical current for a sample having 16.6%  $CeO_2$  as a function of applied field to 150 Gauss is illustrated in Fig. 5. The inset of Fig. 5 is the low field response of a sample having 26%  $CeO_2$ . Both samples had a reduced temperature of 0.9. The result for the 26%  $CeO_2$  sample shows a 40% reduction of  $I_c$  with a 2 Gauss field and supports the theory of Josephson vortex motion rather than weakly pinned Abrikosov vortices. These measurements and results are encouraging for using this material in the development of Josephson vortex flow devices.

## V. SUMMARY AND CONCLUSIONS

We have developed a composite material in which the intergranular coupling between the YBCO grains can be affected by the parameters of the deposition process. These materials were fabricated by off-axis co-sputtering YBCO

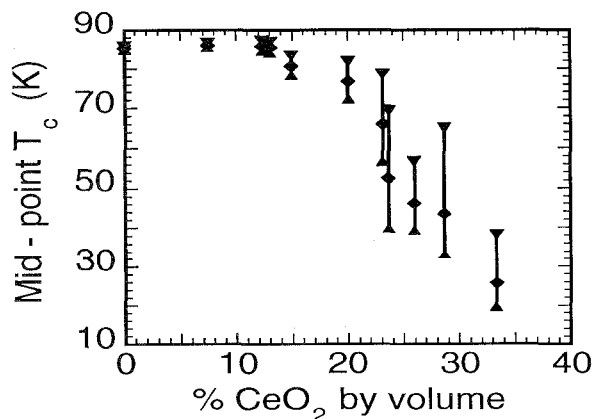


Fig. 3 Resistive midpoint  $T_c$ 's and  $\Delta T_c$ 's of the co-sputtered YBCO/ $CeO_2$  bridges as a function of the % of  $CeO_2$ .

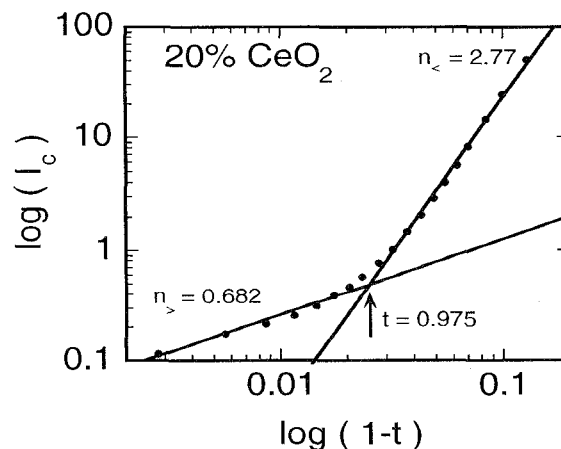


Fig. 4  $\log(I_c)$  vs.  $\log$  bridge showing the two regions of the critical current power law dependence.  $(1-t)$  for a 20%  $CeO_2$

TABLE II  
Properties of Selected Oxygen Plasma Etched YBCO/CeO<sub>2</sub> Bridges

%vol CeO <sub>2</sub>	w (mm)	RR	T <sub>c</sub> (K)	ΔT <sub>c</sub> (K)	R <sub>300K</sub> (Ω)	n <sub>&lt;</sub>	n <sub>&gt;</sub>	t <sub>cross</sub>
0	0.764	2.7	84.5	1.4	27.8	2.43	0.998	0.999
7.4	0.764	2.7	84.4	1.3	39.3	2.44	1.25	0.997
13	0.928	2.2	82.3	2.8	61.6	1.94	1.108	0.991
14.9	1.016	2.0	81.8	2.9	60.7	2.32	0.578	0.993
20	1.583	1.8	75.0	5.7	47.9	2.77	0.682	0.975
23.1	1.911	1.5	51.1	28.6	61.9	1.27	0.399	0.962
26	1.620	1.4	35.4	29.5	106.5	2.03	0.563	0.957
33.3	1.856	1.2	22.8	33.8	179.5	-	-	-
34.4	1.802	1.1	16.5	19.1	890.4	-	-	-

and CeO<sub>2</sub>. We believe this material consists of distorted orthorhombic YBCO grains with Ce incorporated into the crystal lattice for samples with less than 29% CeO<sub>2</sub> while for compositions higher than 33% we observed a new insulating material phase. These YBCO/CeO<sub>2</sub> films have properties characteristic of a two-dimensional array of Josephson-coupled grains.

By increasing the amount of CeO<sub>2</sub> in the film, the superconducting transition temperature was systematically reduced, broadened, and RR decreased. The room temperature resistance increased with CeO<sub>2</sub> composition becoming insulating at high concentrations. Standard photolithographic processing resulted in degradation to the superconducting properties of these composites. However, these properties were restored to values equal to or exceeding those of the as-prepared films by a 20-minute oxygen plasma etch. The temperature dependence of I<sub>c</sub> showed two distinct power law regions with a crossover point in the vicinity of 0.99 T<sub>c</sub> for samples containing smaller amounts of CeO<sub>2</sub>. Samples with the higher concentrations and low T<sub>c</sub> had lower crossover points at approximately 0.95 T<sub>c</sub>. The power law dependence for currents below the crossover temperature was more SNS-like, and above the crossover the slope was more SIS-like. This result would be expected for a two-phase system of interpenetrating superconducting and normal grains. The YBCO/CeO<sub>2</sub> films showed significant I<sub>c</sub> suppression with small magnetic fields suggesting that Josephson vortices are dominating the transport rather than Abrikosov vortices. Magnetic fields of 2 Gauss suppressed I<sub>c</sub>

by 40% in one sample. At lower temperatures, we see a greater reduction in I<sub>c</sub> for the same field, an effect which is unlikely for Abrikosov vortices but compatible with Josephson vortex characteristics. With these magnetic field responses, the YBCO/CeO<sub>2</sub> composite films appear to be promising candidates for the development of three terminal superconducting vortex flow devices.

## REFERENCES

- [1] J.E. Nordman, "Superconductive amplifying devices using fluxon dynamics," *Supercond. Sci. Technol.* 8, pp. 681-699, 1995.
- [2] R. Gerdemann, T. Bauch, O.M. Fröhlich, L. Alf, A. Beck, D. Koelle, and R. Gross, "Asymmetric high temperature superconducting Josephson vortex-flow transistors with high current gain," *Appl. Phys. Lett.* 67, pp. 1010-1012, 1995.
- [3] Y.M. Zhang, D. Winkler, P.A. Nilsson, and T. Claeson, "Flux-flow transistors based on long YBa<sub>2</sub>Cu<sub>3</sub>O<sub>7-δ</sub> bicrystal grain boundary junctions," *Appl. Phys. Lett.* 64, pp. 1153-1155, 1994.
- [4] Kazunori Miyahara, Shugo Kubo, and Minoru Suzuki, "Transresistance and current gain of high-T<sub>c</sub> flux flow transistors," *J. Appl. Phys.* 76, pp. 4772-4775, 1994.
- [5] Laura H. Allen, Edward J. Cukauskas, and Michael A. Fisher, "Thin film composites of Au and YBa<sub>2</sub>Cu<sub>3</sub>O<sub>7-δ</sub>," *Appl. Phys. Lett.* 66, pp. 1003-1005, 1995.
- [6] Michael A. Fisher, Laura H. Allen, and Edward J. Cukauskas, "YBa<sub>2</sub>Cu<sub>3</sub>O<sub>7</sub>/noble metal composite thin films for applications in fluxonic and flux-flow devices," *Appl. Superconductivity*, 3, pp. 607-614, 1995.
- [7] L.H. Allen, and E.J. Cukauskas, "Au/YBa<sub>2</sub>Cu<sub>3</sub>O<sub>7-δ</sub> thin film composites on various substrates," 1996 Applied Superconductivity Conference, Pittsburgh, PA, August, 1996.
- [8] E.J. Cukauskas, Laura H. Allen, R.T. Holm, and Gregory K. Sherrill, "Y<sub>1</sub>Ba<sub>2</sub>Cu<sub>3</sub>O<sub>7-δ</sub> and LaAlO<sub>3</sub> composite thin films by off-axis magnetron sputtering," *Appl. Phys. Lett.* 60, pp. 389-391, 1992.
- [9] A.M.T. Bell, "Calculated x-ray powder diffraction patterns and theoretical densities for phases encountered in investigations of Y-Ba-Cu-O superconductors," *Supercond. Sci. Technol.* 3, pp. 55-61, 1990.
- [10] V. Longo, F. Ricciardiello, and D. Minichelli, "X-ray characterization of SrCeO<sub>3</sub> and BaCeO<sub>3</sub>," *J. Mater. Sci. Lett.* 16, pp. 3503-3505, 1981.
- [11] J.M. Pond, L.H. Allen, and E.J. Cukauskas, "A simple technique for measuring the transition temperature at microwave frequencies," 1996 Applied Superconductivity Conference, Pittsburgh, PA, August, 1996.
- [12] S. Greenspoon and H.J.T. Smith, "Study of the superconducting proximity effects by Josephson tunneling," *Can. J. Phys.* 49, pp. 1350-1360, 1971.
- [13] N.L. Rowell and H.J.T. Smith, "Investigation of the superconducting proximity effect by Josephson tunneling," *Can. J. Phys.* 54, pp. 223-226, 1976.
- [14] J.W.C. de Vries, M.A.M. Gijs, G.M. Stollman, T.S. Baller, and G.N.A. van Veen, "Critical current as a function of temperature in thin YBa<sub>2</sub>Cu<sub>3</sub>O<sub>7-δ</sub> films," *J. Appl. Phys.* 64, pp. 426-429, 1988.
- [15] V. Ambegaokar and A. Baratoff, "Tunneling between superconductors," *Phys. Rev. Lett.* 10, pp. 486-489, 1963; 11, p. 104(E), 1963.
- [16] J. R. Clem, B. Bumble, S. I. Raider, W. J. Gallagher, and Y. C. Shih, "Ambegaokar-Baratoff - Ginzburg-Landau crossover effects on the critical current density of granular superconductors," *Phys. Rev. B*, pp. 66376642, 1987.

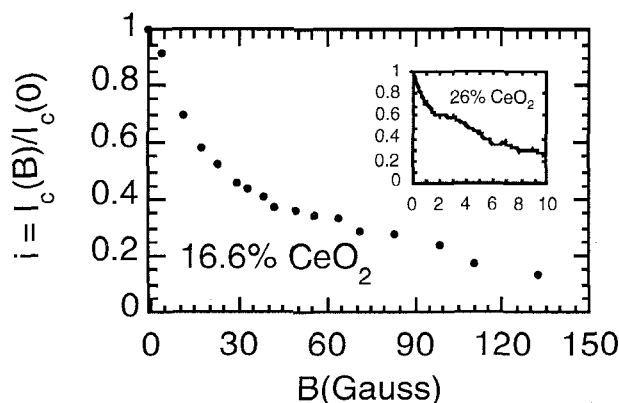


Fig. 5 The magnetic field dependence of I<sub>c</sub> for a 16.6% and 25.9% CeO<sub>2</sub> bridge. The reduced temperature is 0.9.